Biochemical and Biophysical Research Communications 438 (2013) 581–587

Contents lists available at ScienceDirect

Biochemical and Biophysical Research Communications

journal homepage: www.elsevier.com/locate/ybbrc

Influenza A virus (H1N1) increases airway epithelial cell secretion by up-regulation of potassium channel KCNN4

Taryn Waugh [a], John C.H. Ching [a], Yan Zhou [b], Matthew E. Loewen [a,*]

[a] Department of Veterinary Biomedical Sciences, Western College of Veterinary Medicine, University of Saskatchewan, 52 Campus Drive, Saskatoon, SK S7N 5B4, Canada
[b] Vaccine and Infectious Disease Organization, University of Saskatchewan, 120 Veterinary Rd, Saskatoon, SK S7N 5E3,Canada

ARTICLE INFO

Article history:
Received 21 July 2013
Available online 13 August 2013

Keywords:
Ion channels
Airway epithelium
Influenza
CFTR
KCNN4

ABSTRACT

Influenza infects the epithelial cells lining the airways. Normally epithelial cells move solutes through ion channels to create the osmotic drive to hydrate the airways. Viral alteration of this process could explain, in part, the fluid imbalance in the lungs and the resulting pulmonary edema that occurs during severe influenza infections. Using western blot and RT-qPCR, we measured ion channel and cytokine expression in the Calu3 airway cell line after infection with influenza virus (H1N1) for 48 h. We simultaneously measured chloride and potassium channel function by means of a short-circuit current (I_{sc}) produced in an Ussing chamber. At a multiplicity of infection (MOI) of 10, viral M1 protein and pro-inflammatory cytokine expression was observed 24 h post-infection, despite a lack of measurable change in I_{sc}. However, we observed a decreased secretory response in cAMP- and calcium-induced I_{sc} 48 h post-infection. This correlated with a decrease in CFTR and KCNN4 protein levels. Interestingly, a viral dose of an MOI 0.6 revealed an increased secretory response that correlated with pro-inflammatory cytokine expression. This increased secretory response seemed to be primarily driven through KCNN4. We detected an increase in KCNN4 mRNA and protein, while CFTR function and expression remained unchanged. Furthermore, inhibition of the KCNN4-stimulated I_{sc} with TRAM-34, a specific inhibitor, ameliorated the response, implicating KCNN4 as the main driving force behind the secretory phenotype.

1. Introduction

Seasonal circulating strains of influenza A virus cause over half-a-million deaths annually, with mortality rates substantially higher when novel pandemic strains emerge [1]. Influenza-related deaths are primarily due to influenza's ability to disrupt the basic cellular mechanisms of ciliated epithelial cells lining the upper respiratory tract [2]. These cells are normally responsible for regulating the airway surface liquid (ASL), a thin layer of fluid lining the surface of the airways [3]. The ASL, maintained at appropriate volumes, allows the cilia of the epithelium to beat, clearing mucus and inhaled contaminants from the respiratory tract (mucociliary clearance) [4]. The epithelial cells create the ASL by a chloride secretory response that establishes an osmotic gradient across the epithelium [3,5]. This secretory process is driven by the transport of sodium, chloride and potassium through ion channels and pumps [3,6]. Simplistically, potassium exits through ion channels on the apical and basolateral sides of the polarized epithelium, increasing the negative charge within the cell [3,7]. This drives chloride into the airways through apical chloride channels, generating the gradient for both sodium and water to follow [3]. Chloride exits the apical membrane through either the cAMP-activated cystic fibrosis transmembrane regulator (CFTR) channel or calcium-activated chloride channels (CaCC) [3]. The importance of CFTR is illustrated in cystic fibrosis (CF), where CFTR loss results in ASL under-hydration and poor mucociliary clearance [8]. Alternatively, increased movement of chloride through CFTR or CaCC can result in airway over-hydration, pulmonary edema and ultimately suffocation [9]. Such severe pulmonary edema is particularly salient in patients suffering from acute, complicated influenza infections [3,10].

The exact mechanism by which influenza infection can cause the formation of pulmonary edema remains unclear [11]. Initial studies indicate a reduced ability of the epithelium to clear fluid from the airways [10,12–14]. These studies emphasize how down-regulation of the epithelial sodium channel (ENaC) impacts fluid clearance as a direct result of viral attachment [12–14]. Since ENaC is responsible for absorbing sodium, its down-regulation will reduce net absorption of water from the airway leading to pulmonary edema [6].

However, pulmonary edema could also result from increased secretion, rather than decreased absorption. This may be true in most infections where a large percentage of cells are not infected

* Corresponding author.
E-mail address: matthew.loewen@usask.ca (M.E. Loewen).

0006-291X/$ - see front matter © 2013 Elsevier Inc. All rights reserved.
http://dx.doi.org/10.1016/j.bbrc.2013.08.012

Table 1
Primer sequences for RT-qPCR.

Gene name	Forward (5′-3′)	Reverse (5′-3′)	Tm (°C)
GAPDH	CAAGGTCATCCATGACAACTTTG	GGGCCATCCACAGTCTTCTG	60
CFTR	TCCTCCAAACCTCACAGCAACTCA	AAGGCACGAAGTGTCCATAGTCCT	60
KCNN4	GGCCAAGCTTTACATGAACACGCA	AAAGGTGCCCAGTGGCATTAACAG	60
KCNQ1	TCCTCGTACTTTGTGTACCTGGCT	AAAGACAGAGAAGCAGGAGGCGAT	60
NKCC1	CATTAACTGGTGGGCTGCATTGCT	TCACGTGGTCTTCCACTCCAGAAA	60
ATP1A1	GGGCAAATGTCGAAGTGCTGGAAT	TTCCACGGTCTCATTGCCTTCTGA	60
IL-6	AGCCACTCACCTCTTCAGAAC	GTGCCTCTTTGCTGCTTTCAC	57
IL-8	TCTCTTGGCAGCCTTCCTGATTTC	ATTTCTGTGTTGGCGCAGTGTG	60
IL-12α	CAGTGGAGGCCTGTTTACCATTG	TACTACTAAGGCACAGGGCCATC	58
IL-1α	TACCTCACGGCTGCTGCATTAC	GGTCTTCATCTTGGGCAGTCAC	58
IL-1β	GCTGATGGCCCTAAACAGATG	TGTAGTGGTGGTCGGAGATTC	55
TNF-α	TGCTGCACTTTGGAGTGATCG	TGCTACAACATGGGCTACAGG	57

and instead are subject to paracrine regulation by infected neighboring cells [15,16]. Infected epithelial cells respond by releasing a variety of inflammatory mediators that aid in fighting the virus; some inflammatory mediators such as cytokines have been shown to independently increase net anion secretion [17–19]. Such an effect could be mediated through CFTR, CaCC or by increased potassium movement through the major epithelial potassium channels KCNN4 or KCNQ1 [3,7].

To investigate the presence of a secretory response to influenza infection, we used the well-established Calu3 airway epithelial serous cell line [20,21]. In this secretory cell model, chloride is driven through an apical CaCC and highly abundant CFTR after the activation of potassium channels KCNN4 and KCNQ1 [20–22]. Using this model, we determined the dose effect of an influenza virus infection on cytokine and channel expression while simultaneously measuring the secretory response of channel function by Ussing chamber short-circuit current (I_{sc}). Additionally, we modeled the *in vivo* situation where only a percentage of the airway cells were infected, leaving the non-infected cells available for paracrine regulation by virus-induced mediators.

2. Materials and methods

2.1. Cell culture

Calu3 cells at low passage were grown in DMEM (Invitrogen) supplemented with 10% fetal bovine serum (FBS), 1% non-essential amino acids (10 mM), 1% penicillin–streptomycin, 1% sodium pyruvate and 1% L-glutamine (200 mM) at 37 °C in a humidified atmosphere with 5% CO_2. Cells were seeded onto 0.4-μm pore size Snapwells (Corning) and grown in an air–liquid interface for approximately one week prior to infection.

2.2. Viral culture and infection

Influenza A virus (A/PR/8/34 H1N1) was propagated at a multiplicity of infection (MOI) of 0.001 in Madin–Darby canine kidney (MDCK) cells and purified by ultracentrifugation through a sucrose gradient. Virus was diluted in DMEM and added to the apical surface of cells at an MOI of 10, 1, 0.6 or 0.3. Cells were infected or mocked infected apically for an hour, then washed with phosphate buffered saline (PBS) to remove non-adherent virus. Cells were left for 24- or 48-h prior to downstream experiments.

2.3. Measurement of transepithelial I_{sc}

Polarized cells on Snapwells were mounted in Ussing chambers (Physiologic Instruments, San Diego, CA). The apical and basolateral chambers were filled with 5 mL Kreb's solution, maintained at 37 °C and gassed with 5% CO_2-95% O_2, as previously described [21]. Transepithelial potential differences were short-circuited to 0 mV with a voltage clamp on the apical and basolateral chambers using Ag–AgCl electrodes and 3 M KCl agar bridges. A 1 mV pulse and the resulting I_{sc} every 30 s was used to calculate epithelial resistance. Cells were clamped and allowed to equilibrate for a minimum of 20 min.

2.4. Chemicals

All activators and inhibitors were obtained from Sigma and used at the following final concentrations. Forskolin (10 μM; F6886) and IBMX (1 mM; I5879) increases cAMP. A23187 (500 nM; C7522) calcium ionophore. Glibenclamide (100 μM; G0639) CFTR inhibitor. Niflumic Acid (100 μM; N0630) CaCC inhibitor. TRAM-34 (20 μM; T6700) KCNN4 inhibitor.

2.5. RNA isolation and RT-qPCR

RNA was extracted using TRIzol Reagent (15596018; Life Technologies) according to the manufacturer's protocol. mRNA was transcribed into cDNA using GoScript Reverse Transcription system (A5001; Promega). mRNA expression was measured by RT-qPCR using GoTaq qPCR Master Mix (A6002; Promega) with Stratagene MX5000P real-time PCR machines and primers (Table 1).

2.6. Efficiency and fold difference calculation

Dilution series from 1×10^0 fold to 1×10^{-6} fold of cDNA were used to determine the primer efficiency. The C_T value obtained in each dilution was used to generate a linear plot of C_T vs. log copies graph. The efficiency of the primer set is determined with the equation:

$$\text{Efficiency}(\%) = 10^{(-1/\text{slope})}$$

The fold difference between infected and non-infected cells was determined using efficiency corrected calculation model

$$\text{Ratio} = \frac{(\text{Eff}_{\text{target}})\Delta CT\ target\ (\text{Mean control} - \text{Mean sample})}{(\text{Eff}_{\text{ref}})\Delta CT\ \text{ref}\ (\text{Mean control} - \text{Mean sample})}$$

2.7. Western blotting

SDS–PAGE and western blot analysis were carried out as previously described [18,23]. The protein was extracted from Calu3 cells using the NE-PER Nuclear and Cytoplasmic Extraction Reagents (78833; Pierce) and analyzed the same day. Samples were separated by 10% SDS–PAGE, and transferred onto PVDF membranes. After blocking in 5% bovine serum albumin in PBS-Tween for 1 h, membranes were incubated with primary antibody anti-CFTR (1:200; sc-10747; Santa Cruz Biotechnology), anti-KCNN4 (1:200; sc-32949) or anti-GAPDH (1:500; sc-25778) for 2 h. Infrared-labeled secondary antibodies were used to visualize protein.

2.8. Statistical analysis

All data were expressed as mean ± standard error of the mean (SEM). Parametric *t*-tests or ANOVA were used to analyze electrophysiology data. One-sample *t*-tests were performed on RT-qPCR data using fold differences with the mean set at 1. Significance was determined at $p < 0.05$.

3. Results and discussion

3.1. High viral dose 24 h post-infection

To determine the effect of influenza infection and replication on epithelial secretion, we infected polarized Calu3 cell monolayers with H1N1 at an MOI of 10 (i.e., 10 virus particles per cell). The initial use of a high MOI (Figs. 1 and 2) ensured that all cells were infected and allowed us to fully characterize the immune response. Additionally, this dose circumvented any problems associated with pandemic H1N1 eliciting an attenuated immune response as previously reported [24].

Despite the beginnings of a strong immune response and viral replication 24 h post infection, as determined by M1 viral protein production (Fig. 1F), there was no statistical change in epithelial resistance, a measure of epithelial tight junction and cell viability. Infected cells had a resistance of 90.8 ± 8.34 Ωcm^2 whereas non-infected cells had a resistance of 105.3 ± 8.51 Ωcm^2. Additionally, we observed no difference in cAMP-(Forskolin/IBMX) or calcium-induced (A23187) I_{sc}, a measurement of epithelial secretion, between infected and non-infected epithelium (Figs. 1A–D). We expected to detect a change in I_{sc} after 24 h of infection at an MOI of 10, as a previous study reported an impact on sodium absorption within 1 h [12]. However, authors of the previous study only assessed the early stages of viral attachment and endocytosis occurring within a 1-h period [10,12]. These early events did not take into account the dynamic virus-host interactions that occurred upon initiation of viral replication, as the average incubation period for influenza is 24–48 h [1]. Thus, we had predicted that 24 h post-infection would reveal a difference in measurable I_{sc} in addition to increased cytokine levels. However, we only detected significant increases in mRNA of IL-6, IL-8, IL-1α and IL-1β (Fig. 1E) and no change in ion channel function. Since all cells were infected, we concluded that, in our cell model, a longer time was required to observe a measurable difference in ion channel transport. Therefore, we proceeded to assess the impact of virus infection on cells at 48 h post-infection.

3.2. High viral dose 48 h post-infection

At 48 h post-infection, we observed a decreased secretory response, as indicated by a significant decrease in the cAMP- and calcium-activated I_{sc} response from infected cells (Fig. 2A). Also, there was decreased chloride conductance inhibition with glibenclamide (CFTR inhibitor) but not with niflumic acid (CaCC inhibitor) (Fig. 2B). Moreover, the infected epithelial resistance was significantly decreased compared to controls (61.5 ± 7.02 Ωcm^2 and 145.1 ± 21.2 Ωcm^2, respectively; $p = 0.002$). Prolonged influenza exposure has been shown to induce apoptosis [11,16]; therefore, a significant decrease in epithelial resistance, especially at a high dose, was not surprising. Despite detection of a decreased secretory response, the reduction in epithelial resistance indicated a compromised epithelial barrier. The weakening of the epithelium has been suggested to contribute to the development of pulmonary edema as the hydrostatic pressure from the vasculature could then easily force fluid into the airway [5]. Chen et al. discussed that part of the pathogenesis of influenza likely resulted from a damaged epithelial barrier leading to the leakage of fluid into the lungs [14]. This is in contrast to the findings that have demonstrated a direct effect on ion transport by the virus, which may also contribute to pulmonary edema [12].

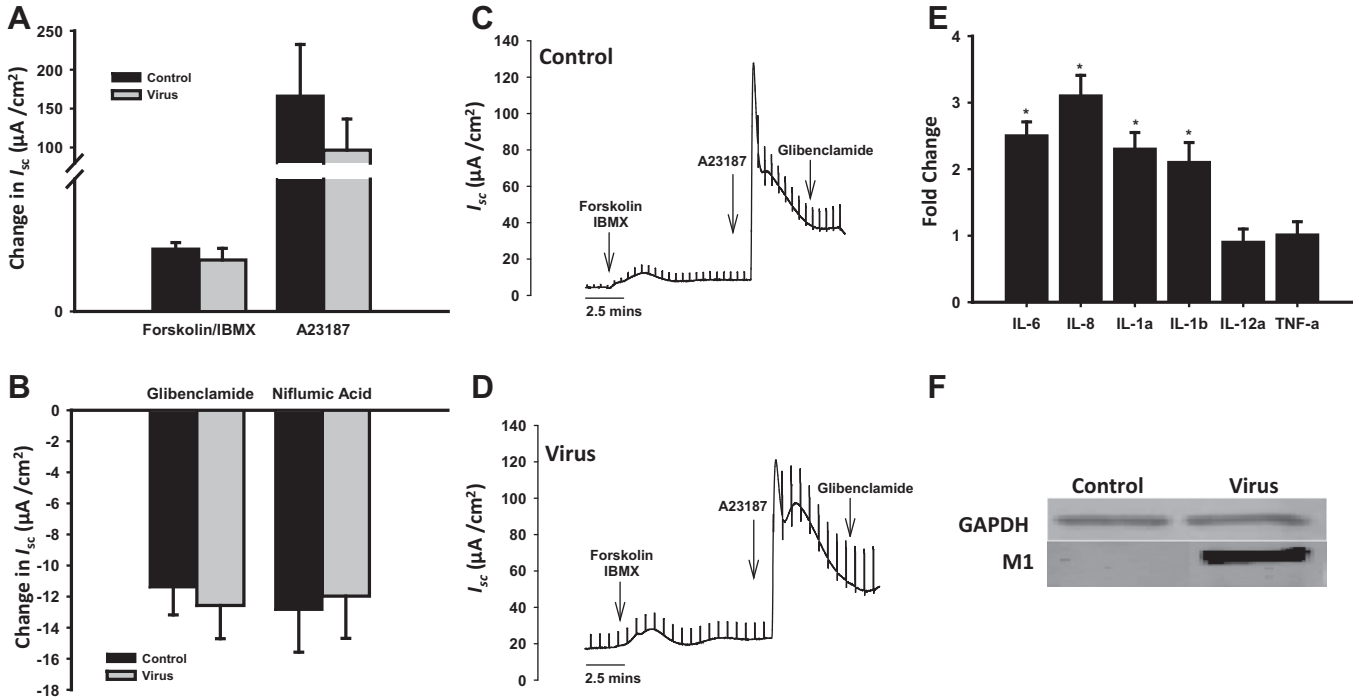

Fig. 1. Effect of high viral dose on Calu3 cells 24 h post-infection. Change in I_{sc} in response to the addition of ion channel activators (A) or inhibitors (B) in control and virus-infected cells (MOI 10) $n = 34$. Experimental I_{sc} traces representing cellular responses to activating and inhibiting drugs among control (C) and virus-infected (D) cells. Change in cytokine mRNA, as measured by RT-qPCR $n = 5$ (E). Western blot of influenza virus M1 protein (~31 kDa) compared to GAPDH (~37 kDa) reference (F). I_{sc} = short-circuit current; Data presented as mean ± SEM and analyzed using parametric *t*-test; $^*p < 0.05$.

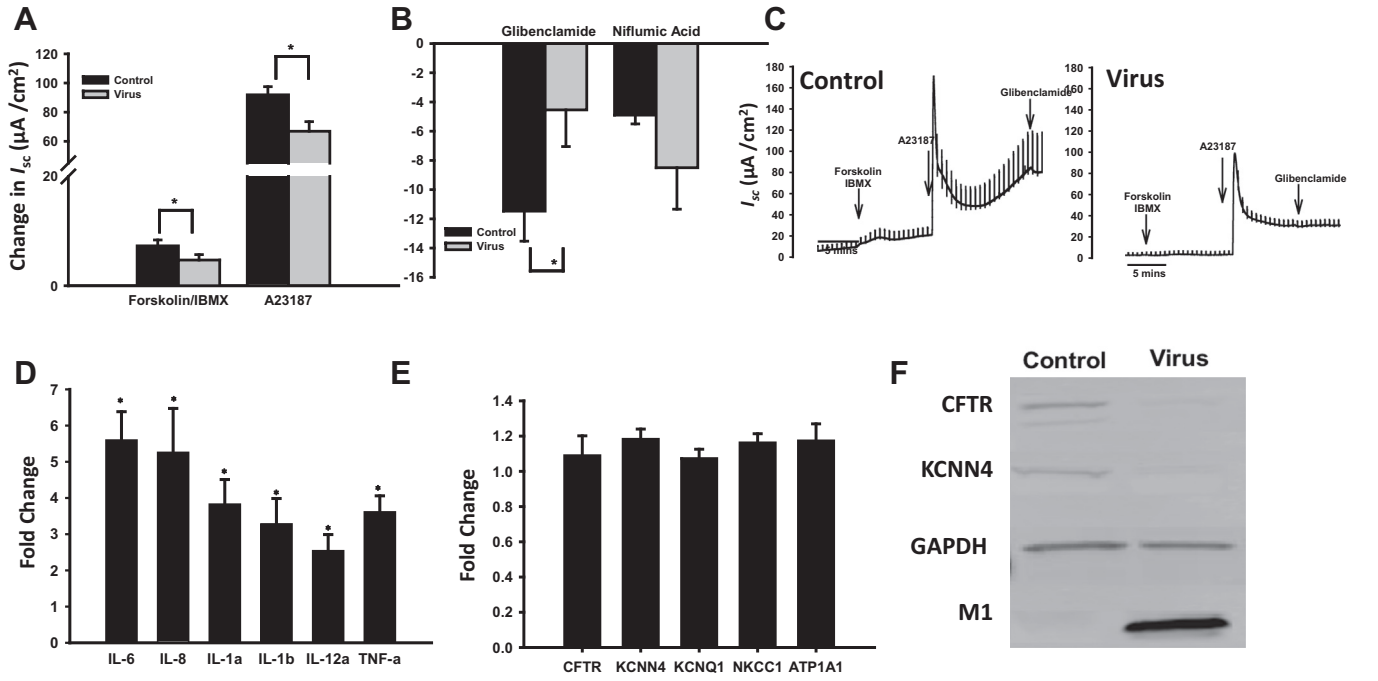

Fig. 2. Effect of high viral dose on Calu3 cells 48 h post-infection. Change in I_{sc} in response to the addition of ion channel activators (A) or inhibitors (B) in control and virus-infected cells (MOI 10) $n = 32$. Experimental I_{sc} traces representing cellular responses to activating and inhibiting drugs among control and virus-infected cells (C). Change in cytokine mRNA (D), and ion channel and transporter mRNA, as measured by RT-qPCR (E) $n = 6$. Representative western blot of CFTR (~150 kDa), KCNN4 (~45 kDa), and influenza M1 protein (~31 kDa) compared to GAPDH (~37 kDa; F). Densitometry normalized to GAPDH ($n = 6$, see text).I_{sc} = short-circuit current; CFTR = cystic fibrosis transmembrane regulator; NKCC1 = $Na^+ - K^+ - 2Cl^-$ cotransporter; ATP1A1 = Na^+ / K^+ ATPase; Data represented as mean ± SEM and analyzed using parametric *t*-test; $^*p < 0.05$.

Interestingly, the decreased secretory 48 h post-infection response was not due to decreased transcription of the transporters responsible for driving secretion. RT-qPCR analysis of mRNA levels for CFTR, KCNN4, KCNQ1 or the basolateral NKCC1 and ATP1A1 were unchanged (Fig. 2E). However, further investigation using western blot indicated a significant reduction in both CFTR (control: 0.87 ± 0.2 OD and virus: 0.1 ± 0.04 OD ($p = 0.002$)) and KCNN4, (control: 0.28 ± 0.07 OD and virus: 0.11 ± 0.065 OD ($p = 0.02$)) protein levels in infected cells (Fig. 2F). Given that mRNA levels remained unchanged, the high viral dose likely induced post-transcriptional modification of both CFTR and KCNN4 resulting in an overall decrease in transepithelial I_{sc}. This could be explained by the viral polymerase subunit cap-snatching of the host's 5′ mRNA caps to transcribe the viral genome [25]. Uncapped host mRNAs would then be targeted for degradation and not transcribed. Despite the fact that there have not been any reports regarding the specificity of the viral polymerase to any host genes, the process may partially explain the reduced ion channel protein expression. Since no change in ion channel mRNA levels was found, the intense viral replication may have masked the up-regulation of mRNA, leaving only changes in protein expression detectable.

Nonetheless, we detected a significant increase in pro-inflammatory cytokine mRNA levels, (Fig. 2D) indicating the virus was capable of eliciting a strong immune response in our cell model. The up-regulation of inflammatory cytokines was a response to fight the viral infection [26]. However, in the airway these same cytokines would exacerbate the inflammatory response that is correlated with increased fluid secretion [10,18,27]. This increased movement of fluid into the airways is likely the result of both the virus and subsequent stimulation of the immune response, inducing changes in ion channel expression [10,12,18]. Both TNF-α and IL-1β have been directly implicated in impairing fluid clearance in the airways [18,28]. Additionally, it should be noted that in most infections, not all of the cells in the airway become infected [15]. This was pointed out by Oh et al. [16], in the context of apoptosis, as lower doses of virus resulted in more non-infected cells that can then be regulated by infected cells in a paracrine fashion. This paracrine regulation could drive the development of pulmonary edema [18,28]. Therefore, we investigated the impact of a lower dose of virus in our cell model, using an MOI of 1 or less to determine whether a particular dose would elicit an increase in secretion.

3.3. Low viral dose response and hypersecretory response

Unexpectedly, when only 30% of the epithelium was infected (MOI 0.3), we observed no detectable changes in ion transport or epithelial resistance 48-h post-infection (Fig. 3A and B). Additionally, this low infectious dose correlated with a relatively low induction of pro-inflammatory cytokine mRNA (Fig. 3G). We speculated that the low MOI of 0.3 was not sufficient to cause a significant paracrine impact on ion channel physiology. However, increasing the dose to an MOI of 1 resulted in a decrease in cAMP- and calcium-activated I_{sc} (Fig. 3E). Additionally, there was a significant decrease in epithelial resistance of infected cells (119.1 ± 14.3 Ωcm^2) compared to non-infected cells (348.2 ± 59.3 Ωcm^2). These results are similar to those resulting from a high viral dose (MOI10). This led us to conclude that once infected with virus, despite any paracrine or autocrine regulation, a cell decreases its secretory response. However, an intermediate dose (MOI 0.6), with a strong inflammatory response, caused a significant increase in the calcium-activated I_{sc} ($p = 0.015$; Fig. 3C). There was no difference in epithelial resistance between infected (189.7 ± 18.1 Ωcm^2) and non-infected (229.3 ± 25.1 Ωcm^2) cells. It is likely that a lower MOI *in vivo* will produce a similar result due to the contribution of immune cells to the paracrine regulation on ion channel function. However, in this model, an MOI of 0.6 with its strong inflammatory

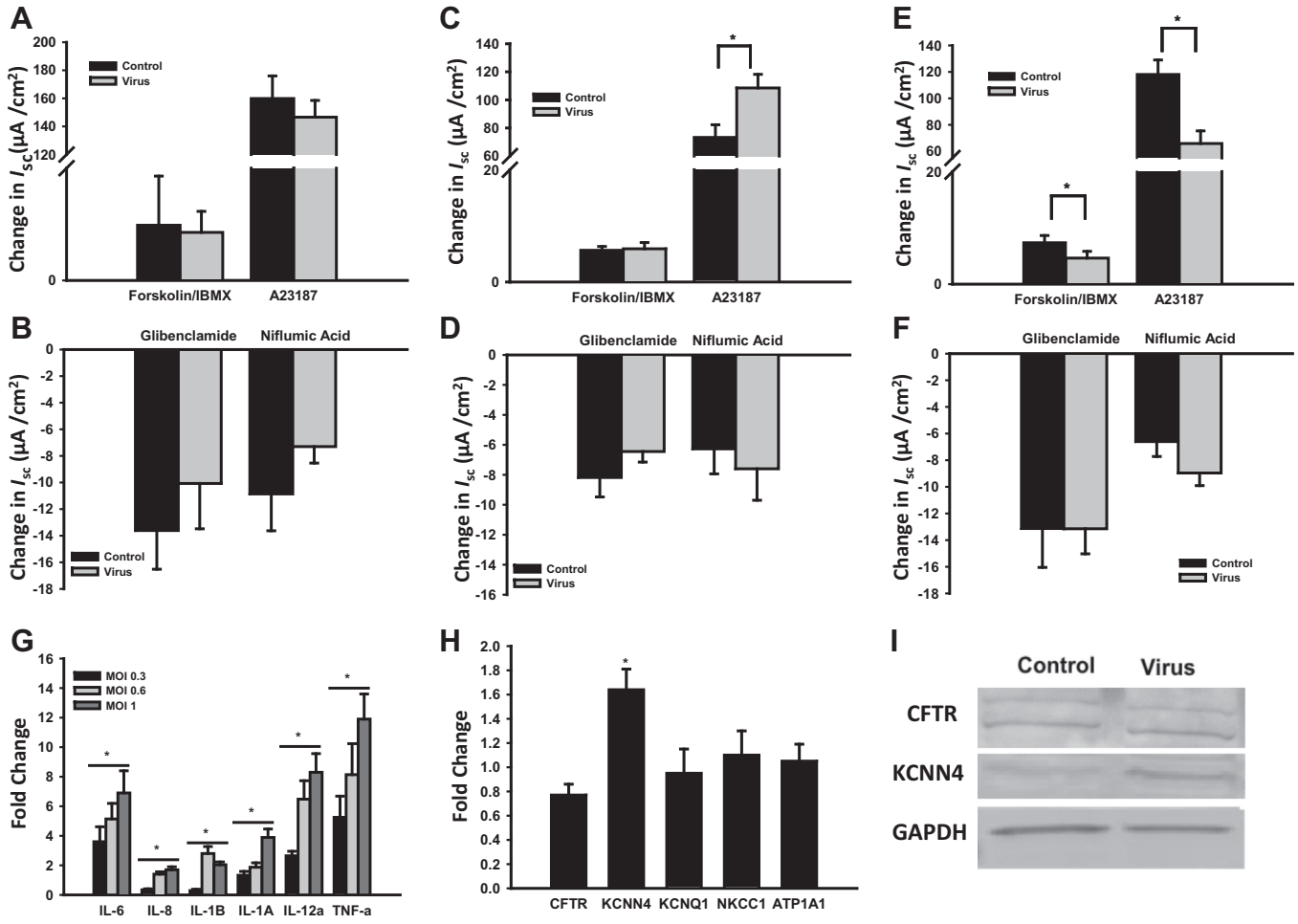

Fig. 3. Viral dose response has varying effect on I_{sc}. Change in I_{sc} in response to the addition of ion channel activators (A, C, E) or inhibitors (B, D, F) in control and virus-infected cells $n = 12$. Virus-infected cells treated with MOIs of 0.3 (A,B), 0.6 (C,D), and 1 (E,F). Change in cytokine mRNA, as measured by RT-qPCR for MOIs 0.3, 0.6 and 1 (G). Change in ion channel and ion transporter mRNA, as measured by RT-qPCR at MOI 0.6, $n = 9$ (H). Representative western blot of CFTR (~150 kDa), KCNN4 (~45 kDa), and GAPDH (~37 kDa) Densitometry normalized to GAPDH ($n = 6$, see text). MOI = multiplicity of infection; I_{sc} = short-circuit current; CFTR = cystic fibrosis transmembrane regulator; NKCC1 = $Na^+ - K^+ - 2Cl^-$ cotransporter; ATP1A1 = Na^+ / K^+ ATPase; Data presented as mean ± SEM and analyzed using parametric t-test; $^*p < 0.05$.

and hypersecretory responses may best model the *in vivo* situation of severe acute influenza infection that results in pulmonary edema.

3.4. KCNN4 drives hypersecretory response

Analysis of the underlying mechanism driving this secretory response revealed that an MOI of 0.6 correlated with an increase in KCNN4 mRNA ($p = 0.005$) and protein (control: 1.02 ± 0.078 OD and virus: 1.45 ± 0.14 OD; $p < 0.001$; Fig. 3H and I). KCNN4, a calcium-activated potassium channel, lowers the membrane potential which drives anion secretion [22]. Up-regulation of this channel would result in an increased drive for apical chloride secretion and movement of fluid into the airways. Additionally, up-regulated levels of CFTR could produce the same results; however, analysis at the mRNA and protein level indicated that CFTR was unchanged (control: 0.93 ± 0.08 OD and virus: 0.87 ± 0.15 OD; Fig. 3H and I).

We confirmed the functional role of KCNN4 by removing its potential contribution to I_{sc} with TRAM-34 [29]. Infected epithelium (MOI 0.6) inhibited with TRAM-34 had significantly reduced calcium-activated I_{sc} compared to non-infected controls ($p < 0.001$; Fig. 4A). Given that KCNN4 mRNA and protein levels were significantly increased over controls, we expected to see a greater degree of inhibition in the infected epithelium. Inhibition of the KCNN4-associated current significantly decreased the overall I_{sc} by 98% in infected cells and 91% in non-infected cells (Fig. 4A). This study demonstrated that in our cell model when 60% of the epithelium was infected, the driving force for chloride secretion was increased, as a result of up-regulated levels of KCNN4. This channel may be only partially responsible for this secretory response, but our data suggested that KCNN4 was the primary channel responsible for the increased calcium-activated I_{sc}. Such a mechanism involving KCNN4 up-regulation, if occurring in vivo, could ultimately contribute to the formation of pulmonary edema through an increased driving force for chloride into the airways.

Detection of an increased secretory response during influenza infection and identification of the key ion channel driving the response will undoubtedly open a new area of pharmacotherapy. Our study is the first to identify KCNN4 as a potential target for drug therapy to reduce the severity of H1N1 infections with regards to pulmonary edema formation. Although further mechanistic investigations are required to understand the interaction between influenza and KCNN4, the work presented here clearly points to a new avenue to improve the outcome of patients suffering from severe influenza infections.

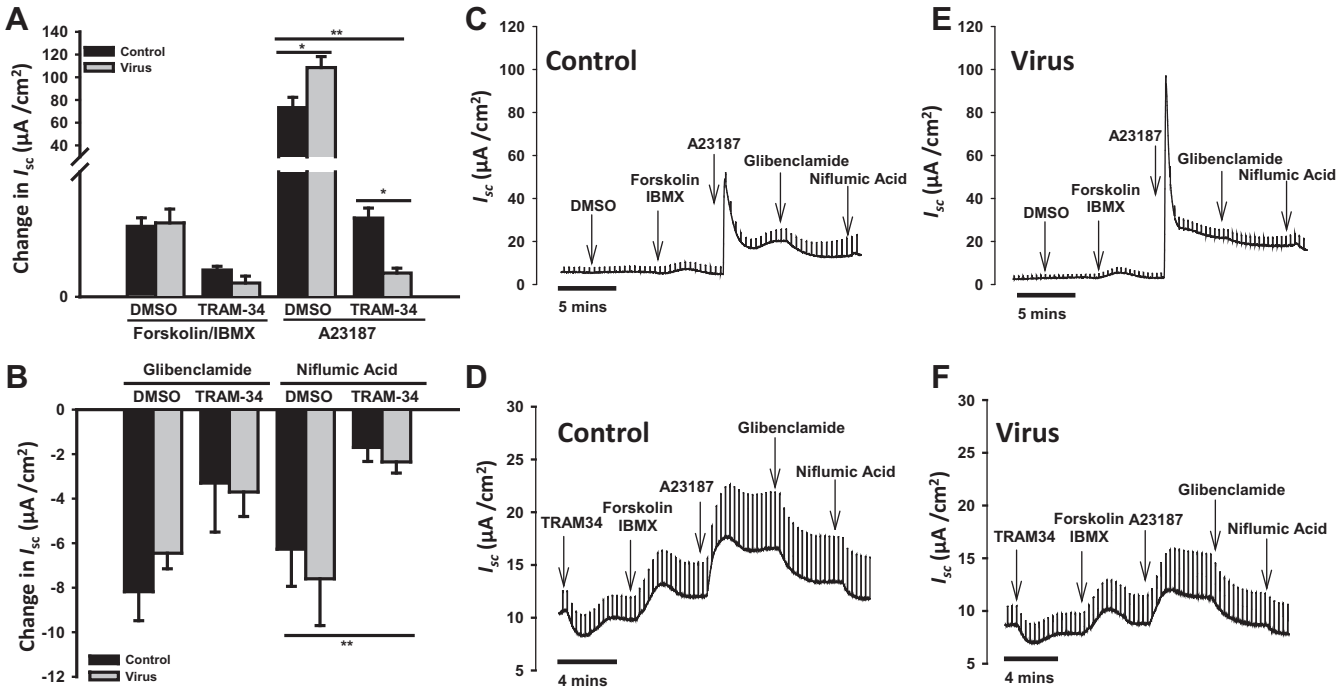

Fig. 4. TRAM-34 inhibition reduces calcium-stimulated I_{sc} in Calu3 cells infected at MOI 0.6. Change in I_{sc} in response to the addition of ion channel activators (A) or inhibitors (B) in control and virus-infected cells exposed to the KCNN4 inhibitor TRAM-34 or DMSO, $n = 10$. Experimental I_{sc} traces representing cellular responses to activating and inhibiting drugs among control cells exposed to DMSO control (C) or TRAM-34 inhibitor (D) and virus-infected cells exposed to DMSO control (E) or TRAM-34 inhibitor (F). I_{sc} = short-circuit current; Data presented as mean ± SEM and analyzed using two-way ANOVA with interaction term; $^{*}p < 0.05$; $^{**}p < 0.001$.

Acknowledgments

The work was supported by the Natural Sciences and Engineering Research Council of Canada Discovery Grant 371364-2010 (M.E.L.), a Saskatchewan Health Research Foundation New Investigator Grant (M.E.L.), an Equine Health Research Fund Grant as well as a Canada Foundation for Innovation Grant 24021 (M.E.L.).

References

[1] CDC, Prevention and control of influenza, MMWR 57 (2008) 1–8.
[2] D. Bruder, A. Srikiatkhachorn, R.I. Enelow, Cellular immunity and lung injury in respiratory virus infection, Viral Immunol. 19 (2006) 147–155.
[3] M.I. Hollenhorst, K. Richter, M. Fronius, Ion transport by pulmonary epithelia, J. Biomed. Biotechnol. 2011 (2011) 174306.
[4] M.B. Antunes, N.A. Cohen, Mucociliary clearance – a critical upper airway host defense mechanism and methods of assessment, Curr. Opin. Allerg. Clin. Immun. 7 (2007) 5–10.
[5] D.C. Eaton, M.N. Helms, M. Koval, et al., The contribution of epithelial sodium channels to alveolar function in health and disease, Annu. Rev. Physiol. 71 (2009) 403–423.
[6] M. Althaus, W.G. Clauss, M. Fronius, Amiloride-sensitive sodium channels and pulmonary edema, Pulm. Med. 2011 (2011) 830320.
[7] S.L. Moser, S.A. Harron, J. Crack, et al., Multiple KCNQ potassium channel subtypes mediate basal anion secretion from the human airway epithelial cell line Calu-3, J. Membr. Biol. 221 (2008) 153–163.
[8] M. Briel, R. Greger, K. Kunzelmann, Cl- transport by cystic fibrosis transmembrane conductance regulator (CFTR) contributes to the inhibition of epithelial Na^+ channels (ENaCs) in Xenopus oocytes co-expressing CFTR and ENaC, J. Physiol. 508 (Pt 3) (1998) 825–836.
[9] G.M. Mutlu, J.I. Sznajder, Mechanisms of pulmonary edema clearance, Am. J. Physiol. Lung Cell Mol. Physiol. 289 (2005) L685–695.
[10] K.E. Wolk, E.R. Lazarowski, Z.P. Traylor, et al., Influenza A virus inhibits alveolar fluid clearance in BALB/c mice, Am. J. Respir. Crit. Care Med. 178 (2008) 969–976.
[11] C. Sartori, M.A. Matthay, Alveolar epithelial fluid transport in acute lung injury: new insights, Eur. Respir. J. 20 (2002) 1299–1313.
[12] K. Kunzelmann, A.H. Beesley, N.J. King, et al., Influenza virus inhibits amiloride-sensitive Na^+ channels in respiratory epithelia, Proc. Natl. Acad. Sci. USA 97 (2000) 10282–10287.
[13] A. Lazrak, K.E. Iles, G. Liu, et al., Influenza virus M2 protein inhibits epithelial sodium channels by increasing reactive oxygen species, FASEB J. 23 (2009) 3829–3842.
[14] X.J. Chen, S. Seth, G. Yue, et al., Influenza virus inhibits ENaC and lung fluid clearance, Am. J. Physiol. Lung Cell Mol. Physiol. 287 (2004) L366–373.
[15] N. Nakajima, Y. Sato, H. Katano, Histopathological and immunohistochemical findings of 20 autopsy cases with 2009 H1N1 virus infection, Mod. Pathol. 25 (2012) (2009) 1–13.
[16] S. Oh, J.M. McCaffery, M.C. Eichelberger, Dose-dependent changes in influenza virus-infected dendritic cells result in increased allogeneic T-cell proliferation at low, but not high, doses of virus, J. Virol. 74 (2000) 5460–5469.
[17] J. Roux, H. Kawakatsu, B. Gartland, et al., Interleukin-1beta decreases expression of the epithelial sodium channel alpha-subunit in alveolar epithelial cells via a p38 MAPK-dependent signaling pathway, J. Biol. Chem. 280 (2005) 18579–18589.
[18] A. Dagenais, R. Frechette, Y. Yamagata, et al., Downregulation of ENaC activity and expression by TNF-alpha in alveolar epithelial cells, Am. J. Physiol. Lung Cell Mol. Physiol. 286 (2004) L301–311.
[19] L.J. Galietta, C. Folli, C. Marchetti, et al., Modification of transepithelial ion transport in human cultured bronchial epithelial cells by interferon-gamma, Am. J. Physiol. Lung Cell Mol. Physiol. 278 (2000) L1186–1194.
[20] J. Shan, J. Huang, J. Liao, et al., Anion secretion by a model epithelium: more lessons from Calu-3, Acta Physiol. (Oxf) 202 (2011) 523–531.
[21] B.Q. Shen, W.E. Finkbeiner, J.J. Wine, et al., Calu-3: a human airway epithelial cell line that shows cAMP-dependent Cl- secretion, Am. J. Physiol. 266 (1994) L493–501.
[22] E.A. Cowley, P. Linsdell, Characterization of basolateral K+ channels underlying anion secretion in the human airway cell line Calu-3, J. Physiol. 538 (2002) 747–757.
[23] E. Brochiero, A. Dagenais, A. Prive, et al., Evidence of a functional CFTR Cl(-) channel in adult alveolar epithelial cells, Am. J. Physiol. Lung Cell Mol. Physiol. 287 (2004) L382–392.
[24] H. Zeng, C. Pappas, J.M. Katz, The 2009 pandemic H1N1 and triple-reassortant swine H1N1 influenza viruses replicate efficiently but elicit an attenuated inflammatory response in polarized human bronchial epithelial cells, J. Virol. 85 (2011) (2009) 686–696.
[25] A. Dias, D. Bouvier, T. Crepin, et al., The cap-snatching endonuclease of influenza virus polymerase resides in the PA subunit, Nature 458 (2009) 914–918.
[26] T.M. Tumpey, A. Garcia-Sastre, J.K. Taubenberger, Pathogenicity of influenza viruses with genes from the 1918 pandemic virus: functional roles of alveolar macrophages and neutrophils in limiting virus replication and mortality in mice, J. Virol. 79 (2005) (1918) 14933–14944.

[27] S. Matsukura, F. Kokubu, H. Noda, et al., Expression of IL-6, IL-8, and RANTES on human bronchial epithelial cells, NCI-H292, induced by influenza virus A, J. Allergy Clin. Immunol. 98 (1996) 1080–1087.
[28] T. Gray, R. Coakley, A. Hirsh, et al., Regulation of MUC5AC mucin secretion and airway surface liquid metabolism by IL-1beta in human bronchial epithelia, Am. J. Physiol. Lung Cell Mol. Physiol. 286 (2004) L320–330.
[29] H. Wulff, N.A. Castle, Therapeutic potential of KCa3.1 blockers: recent advances and promising trends, Expert Rev. Clin. Pharmacol. 3 (2010) 385–396.